Field Study of Pre-Breakup River Waves

Spyros Beltaos and Robert Rowsell
National Water Research Institute, Burlington, Ontario
867 Lakeshore Road, Burlington, Ontario, L7R 4A6
Spyros.Beltaos@CCIW.ca Bob.Rowsell@CCIW.ca

River waves under an ice cover have been studied in recent theoretical works. It has been postulated that certain types of small-amplitude waves, as may occur shortly before breakup, can generate sufficient bending moments to fracture the cover. However, the period of such waves is too short to "register" in standard water-level gauge recordings and there is no evidence as to their existence and properties. Using specially designed instrumentation, a first attempt to record the passage and characteristics of pre-breakup river waves was made in March 2000, on the S.W. Miramichi River, NB. During the three-day monitoring interval, extending to a few hours before local breakup initiation, numerous waves were recorded, with amplitudes and periods of 0.5-2.0 cm, and 70-300 s, respectively. Typically, the waves occurred in sets of three or four similar, though not identical, sinusoidal forms. Using local hydraulic data, it was estimated that the recorded waves were in the gravity band with wavelengths between 270 and 1500 m. Using previous theoretical formulations, it was found that the observed waves were too "flat" to fracture the ice cover. It is planned that future measurements include simultaneous recordings with two transducers, to permit direct determination of wave celerity; and extend right through the breakup event to also record waves that may result from ice-jam releases.

1. Introduction

The breakup of the i.e. cover in Canadian rivers is a brief but crucial event in the life cycle of many aquatic species. At the same time, the breakup can trigger extreme ice-jam events with major socio-economic impacts. The need for science–based understanding of river ice breakup processes, known to be intimately linked to hydroclimatic factors, is accentuated by the emerging issue of climate change. Predicting, and adapting to, climate impacts on our aquatic ecology and economy, via alterations to ice breakup regimes, requires a thorough and quantitative knowledge of the complex mechanisms that are at work. Of these, the mechanisms that govern the onset of breakup play a central role, and have been the object of many previous studies (e.g. see Beltaos, 1995, 1997). In the past decade, it has been possible to depart from the empiricism of earlier works, and derive a conceptual model that has been shown to be free from site-specific data requirements, and applicable to different sites with minimal calibration. The quantification of this model depends on the spacing of transverse cracks, which form after longitudinal, near-bank, fractures (known as "hinge" cracks) appear, and before the ice cover is

set in motion (Beltaos, 1997). Typically, transverse cracks are spaced a few river widths, or hundreds of metres, apart, and are thought to result from flexure due to bending on horizontal and vertical planes.

Significant vertical bending can be induced by, among other causes, high-frequency, low-amplitude water waves travelling under an ice cover, and has been proposed as a possible cracking mechanism (Daly, 1993, 1995). However, such waves cannot be "perceived" by conventional water level gauges owing to relatively coarse time resolution, and no relevant data seem to have ever been obtained. To determine whether waves of this kind actually occur in rivers during the pre-breakup phase, and to measure their characteristics, specially designed equipment was deployed on the Southwest Miramichi River in March 2000. The results of the monitoring activities are reported herein.

2. Background Information

The propagation of water waves under an ice cover has been studied by numerous investigators, especially with respect to deep-water, sea-ice applications (e.g. see Balmforth and Craster, 1999). For ice-covered rivers, Daly (1993) presented a mathematical analysis that was further refined in a discussion by Steffler and Hicks (1994). The sources of under-ice river waves "cannot be identified positively" but they have to originate at water surface disturbances of various types. These may include surges from ice jam releases, reservoir releases, or even brief movements of individual ice sheets. Assuming sinusoidal water and flexural waves propagating in phase under and within, an infinitely long ice cover, Daly determined the wave celerity as a function of channel characteristics and ice properties. This variation is illustrated in Fig. 1 for waves advancing in the downstream direction (*positive* waves). The diagrams in Fig. 1 show how the celerity, C, normalized with the average unperturbed-flow velocity, V, varies with the dimensionless wave number, defined as $2\pi y/SL$ (y = under-ice water depth, S = river slope, and L = wavelength). Different behaviour is exhibited within different ranges, or 'bands", depending on wavelength, river slope, and flow depth.

The first band comprises very small wave numbers (or very large wavelengths, L) and is known as the *kinematic* band. Here, gravitational and frictional forces are dominant, while the celerity, C, is constant, and approximately equal to 1.5V. Kinematic waves propagate only in the downstream direction (Ponce and Simons, 1977). In the second, or *dynamic* band, C increases with wave number as inertial forces also play a role. Inertial and gravitational forces dominate the third, or *gravity*, band. The celerity is again constant but much higher than the kinematic value:

$$C = \left| V \pm \sqrt{gy} \right| \qquad \text{(gravity band)} \qquad (1)$$

The plus and minus signs in Eq. 1 correspond to waves that respectively propagate in the downstream and upstream directions.

The gravity band is followed by the *ice-coupled* band, where gravitational, inertial, and ice-bending forces predominate. The celerity increases with increasing wave number in the ice-coupled band, and becomes a constant in the final, or *acoustic*, band. It may be seen in Fig. 1 that C does not

depend on ice properties in the first three bands, thus behaving much as it would in an open channel (see also Ponce and Simons, 1977).

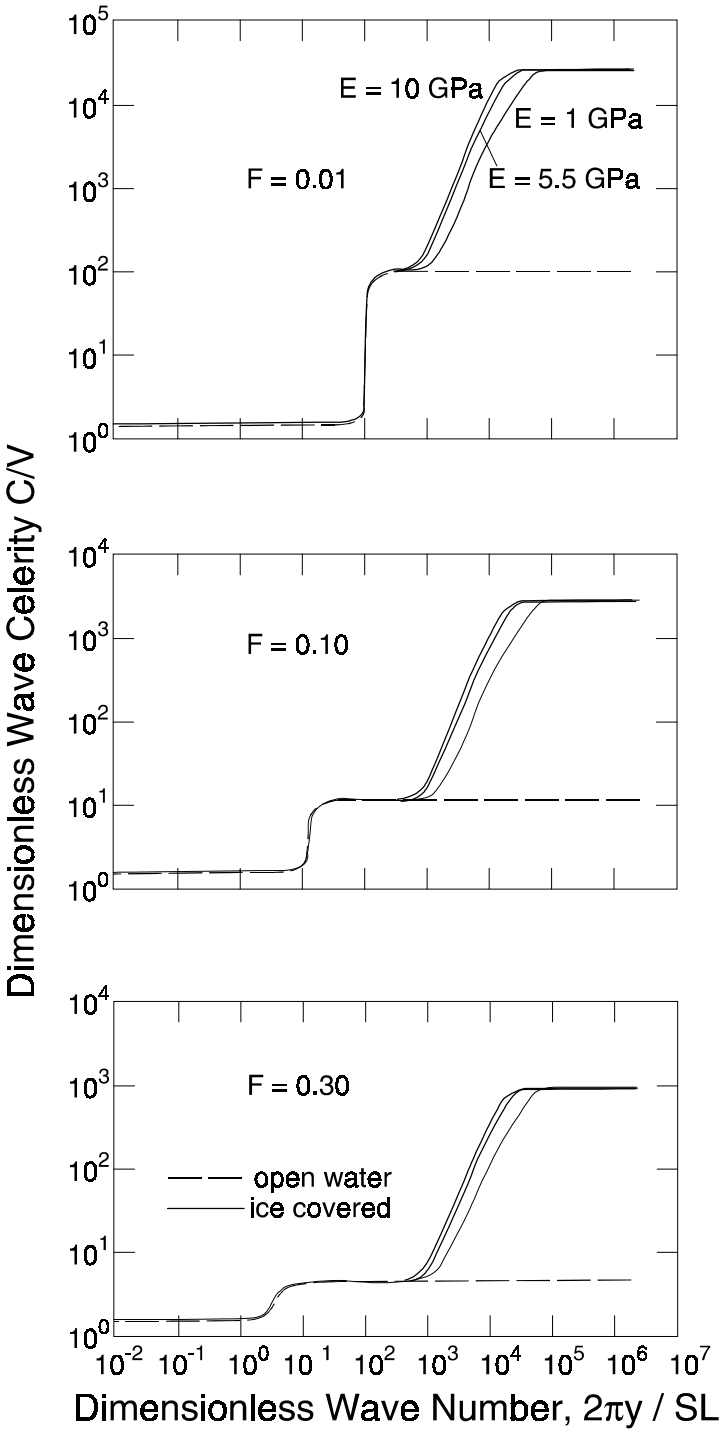

Fig. 1. Variation of wave celerity with wave number, as a function of flow and ice properties (after Daly, 1993, with changes). F = Froude number, E = modulus of elasticity of ice.

In a later paper, Daly (1995) investigated the conditions under which an ice cover could be fractured by water waves. This was done in terms of the characteristic length of the ice cover, ℓ, which is defined by:

$$\ell = \sqrt[4]{\frac{Eh_i^{\,3}}{12(1-\nu^2)\gamma}} \qquad (2)$$

in which h_i = ice cover thickness; γ = unit weight of water; and ν = Poisson ratio for ice $\approx 1/3$. Daly's analysis (1995) resulted in the following conclusions:

-Long waves ($L/\ell >> 2\pi$) are not very effective in fracturing the ice cover, which is consistent with the theoretical results of Billfalk (1982) and Beltaos (1990) who had ignored (as small) the vertical acceleration effects on ice flexure.

-Short waves ($L/\ell << 2\pi$) are also ineffective in fracturing an ice cover.

-Wavelengths near $2\pi\ell$ are the most effective, being capable of fracturing the ice cover even with moderate amplitude (e.g. 0.05-0.20 m). The wave period associated with this range of L is estimated to be between 0.2 and 20 seconds, far too short to be discerned in records of ordinary hydrometric gauges.

More recently, Xia and Shen (1999) presented a theoretical analysis of non-linear waves and concluded that highly asymmetrical "cnoidal" waves would be more effective in fracturing the ice cover than sinusoidal ones. This is not surprising because cnoidal waves are characterized by brief, sharp peaks (or troughs) separated by prolonged, flat troughs (or peaks). As evidence in support of their theory, the authors noted that theoretically derived wavelengths were comparable to observed distances between transverse cracks in river ice covers (typically hundreds of metres).

3. Instrumentation and Site Characteristics

A site was selected along the Southwest Miramichi River near Howard Ferry, approximately halfway between the Blackville hydrometric gauging station, operated by Water Survey of Canada, and the Upper Blackville Bridge (Fig. 2). Early hinge cracks and an open-water strip along the north shore, together with an elevated small field nearby, provided an ideal site for locating the logging system (Fig. 3). The monitoring site is located in a relatively straight and regular reach of the river, as illustrated in Fig. 4.

A Campbell Scientific CR23X micrologger was used to collect climate data (Air Temperature, Relative Humidity, Barometric Pressure, Wind Speed and Direction) from a 3 metre mast over ten-minute periods. In addition to this, the logger also recorded water level data at 2 Hz from a Druck PDCR 1830-8335 pressure transducer, placed in a bottom mount near shore (Fig. 5). Data were recorded on two external storage modules and the data were downloaded to a PC daily. The 1830 transducer units have a polyurethane vented cable which vents the diaphragm to the surface so that measurements do not have to be corrected for changes in barometric pressure.

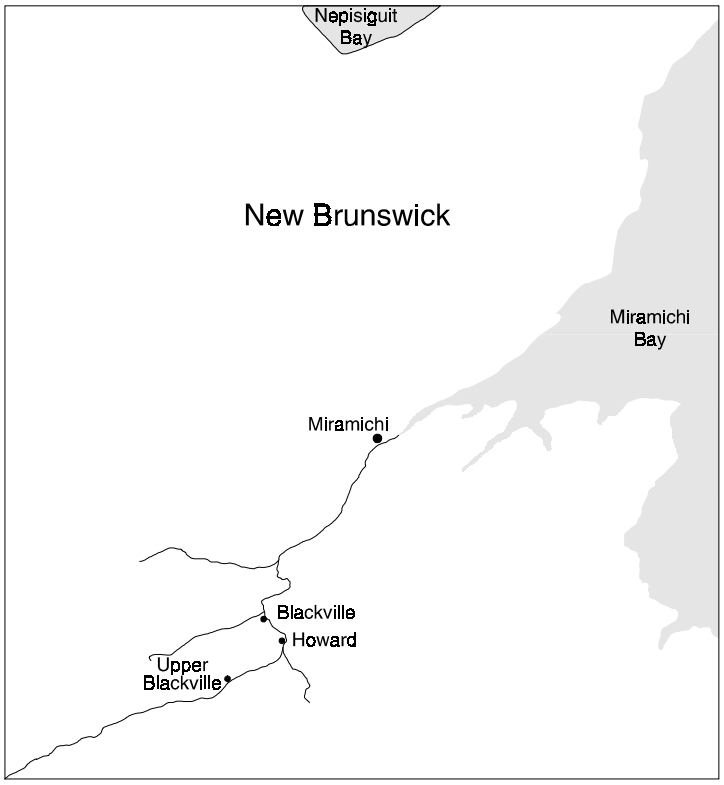

Fig. 2. Plan of lower Southwest Miramichi River and location of wave meter instrumentation.

Fig. 3. Instrumentation deployment site. Looking toward the right (South) bank of the river. Left-Right bank convention is for an observer facing downstream.

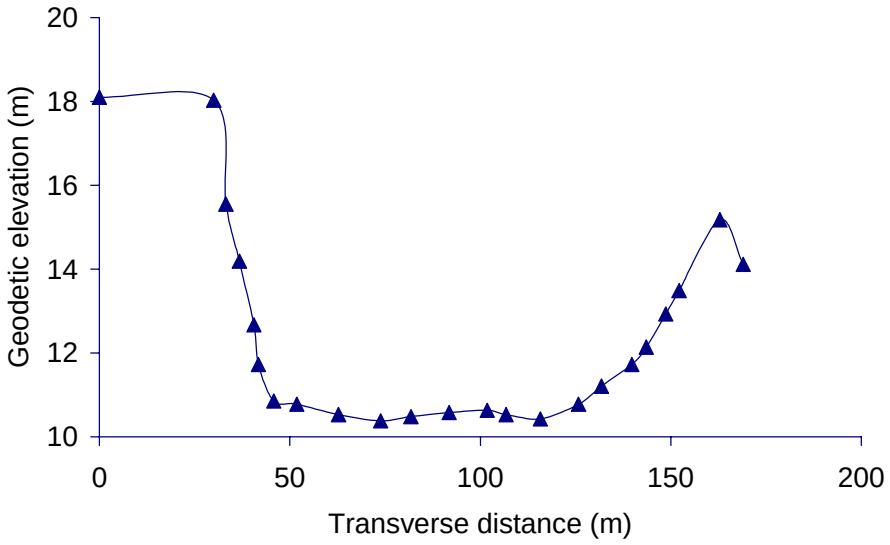

Fig. 4. Cross-section of S.W. Miramichi River near the measurement site.

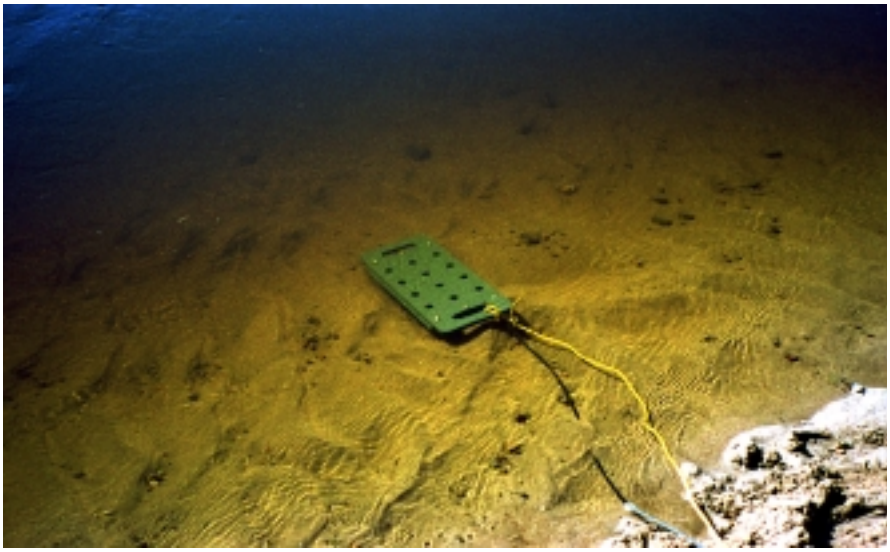

Fig. 5. Transducer (in its protective casing), placed under water near the riverbank in open water strip near the left (North) riverbank.

The pressure transducer had a manufacturer's full-scale pressure range of 5 psig (34.48 kPa or 3.5 m of water). Because the logger only provided 5 volts of excitation (half of what is specified by Druck) the full-range output was cut in half, thus doubling the resolution to 0.1 mm. This value was sufficiently low to be considered acceptable for the intended measurements. The

manufacturer-supplied transducer calibration was tested and slightly adjusted at the National Water Research Institute prior to deployment, resulting in a transducer error of ±0.8 mm. The overall error of measurement includes the data logger error (0.07 mm) and is thus under ±1 mm. The effect of temperature on the calibration of the transducer can be determined using specifications provided by the manufacturer. It can be significant if the parameter of interest is the immersion depth. Where the main interest is in water surface perturbations, such as waves, the effect is negligible (0.25%).

4. River Ice Conditions

The wave meter was installed in the morning of March 26, 2000 and was removed in the afternoon of March 29, shortly before breakup of the local ice cover. Due to a malfunction of the recording system, data are missing for the period starting at 1530 h, March 27 and ending at 1420 h, March 28. The river was first inspected in late afternoon of March 25 from various river access points on the ground, and at that time the ice cover was in good condition throughout the study reach. Hinge cracks had already developed but no transverse cracks were noticed. A day later, i.e. in the afternoon of March 26, several transverse cracks were observed from the ground. Aerial reconnaissance on the following day (1200 – 1300 h, March 27) revealed numerous such cracks, spaced at varying distances, and commonly in the range 200 – 300 m (see also Fig. 6). There were also reaches, several kilometres long, where no transverse cracks were present. The wave meter record showed no waves from the time of installation until 10:33 h, March 27, when a single wave was recorded at 10:33 h. This was followed by a two-crest wave at 11:53 h, and by several wave trains during 12:14 – 14:00 h. More wave episodes were recorded on March 28 and 29.

Fig. 6. Aerial view of river illustrating transverse cracks

5. Wave Characteristics

The pressure recorded by the transducer describes the water wave propagating under the ice cover. The ice cover deforms in phase with this pressure, but with a different amplitude (Daly, 1995). It is assumed that the pressure wave form is two-dimensional, hence the recorded hydraulic head is representative of the entire cross-section. This is a reasonable assumption for a straight river reach, where the waves have traveled for some distance from their point of origin.

Typical pressure recordings are shown in Figs. 7a to 7c, illustrating various types of waves. Of these, the most relevant is Fig. 7a, which depicts "significant" waves, herein defined as waves with amplitudes in excess of 1 cm. Small (amplitude < 1 cm) waves are shown in Figs. 7b and 7c. From simultaneous wind speed and direction measurements, it has been determined that the high-frequency waves of Fig. 7c are ripples that occurred when the wind was strong and blowing along the channel direction.

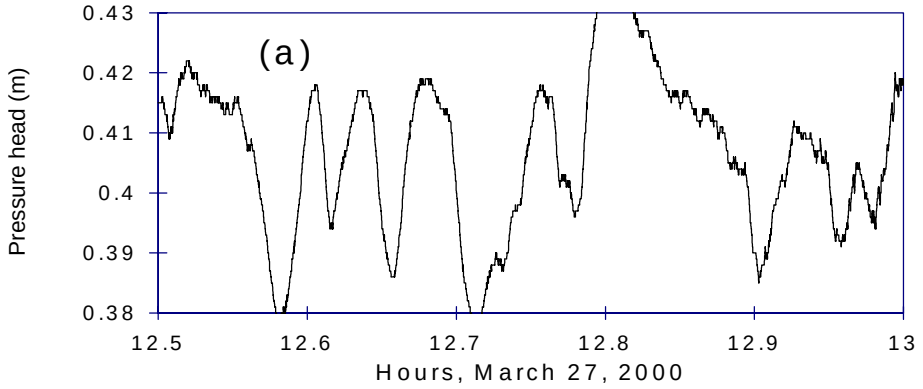

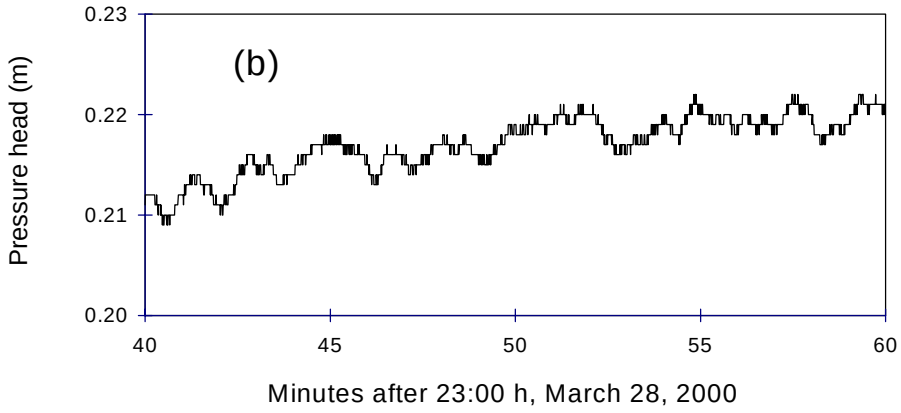

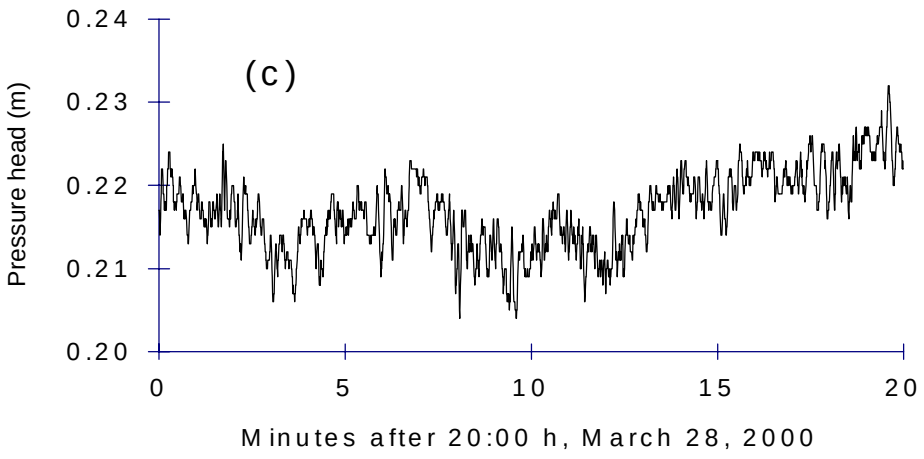

Fig. 7. Example of: (a) “significant” waves; (b) small waves; and (c) wind-ripples

Careful inspection of the entire record revealed the following features for the significant type of wave:

1. The wave forms do not exhibit consistent bias with respect to horizontal and vertical orientation: the shapes of the waves do not change when the vertical axis orientation is inverted, while the average slopes of rising and falling limbs are not statistically distinguishable.

2. The wave forms are approximately sinusoidal in shape, but individual waves within a sequence are not identical (Fig. 8).

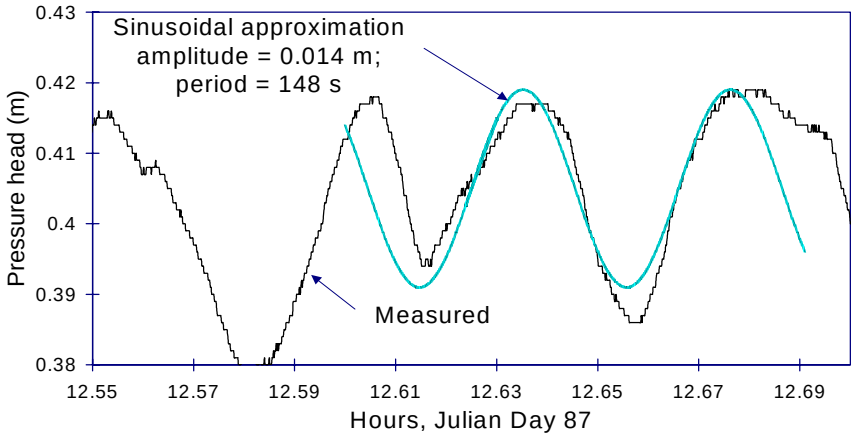

Fig. 8. Sinusoidal fit to one of the wave forms in a sequence

A broad positive correlation between wave amplitude and period was also noticed, as illustrated in Fig. 9. The significance of this correlation is not known at present, but could be related to the wave generation process, as discussed later. In general, the present data indicate that the wave period ranges from about 70 s to 320 s. The right-most point in Fig. 9 (T = 444 s) does not seem to belong with the rest and is considered an outlier.

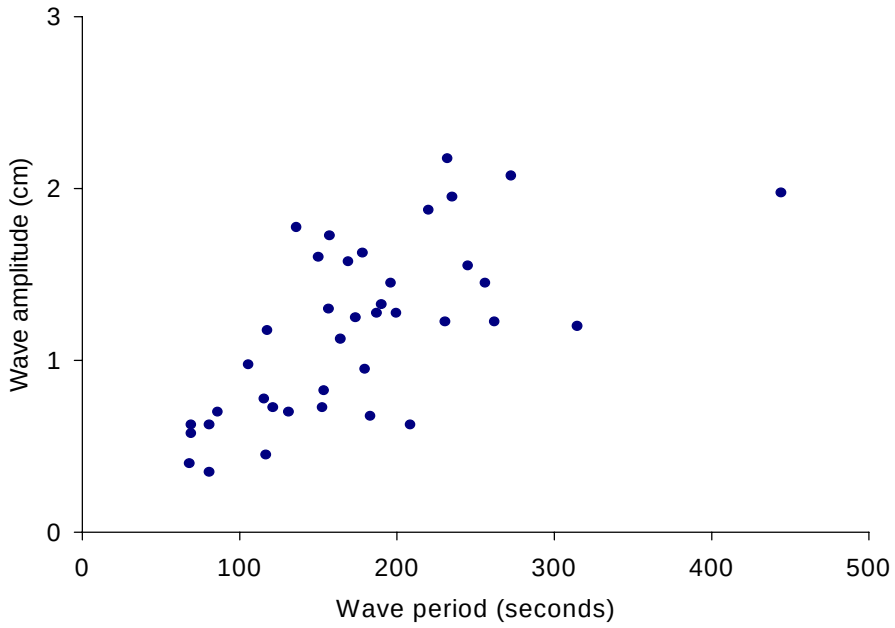

Fig. 9. Relationship between amplitude and period

6. Preliminary Analysis

6.1. Determination of Wavelength

The first question that arises from the data review concerns the magnitude of the wavelength associated with the recorded waves. Since the measurements were carried out at a single site, the wavelength, L, can only be calculated using the measured wave period, T, and estimated wave celerity, C, i.e.:

$$L = CT \qquad (3)$$

Figure 1 indicates that C depends on the average flow velocity, V, as well as on L, under-ice depth, y, and river slope, S. From local water - level and bathymetric data (e.g. Fig. 4), S has been determined as 0.374 m/km, while y is estimated to have ranged between 1.75 and 1.97 m during the period of the wave measurements. Using preliminary flow estimates at the Blackville gauge, provided by Water Survey of Canada, and prorating the flow at the wave metering site according to drainage basin area, V is estimated as 0.38-0.50 m/s. The corresponding range of

the Froude number is 0.09-0.11, while the kinematic- and gravity-band ranges of C are $C_{kin} \approx 0.6$ - 0.75 m/s and $C_{grav} \approx |4.27 \pm V|$ m/s. These ranges are sufficiently narrow to permit use of single, average values, i.e.:

$V \approx 0.44$ m/s, $F \approx 0.10$, $C_{kin} \approx 0.68$ m/s, $C_{grav} \approx 3.8$ or 4.7 m/s (up- or down- stream propagation)

Using these values, and T = 70 to 320 s (Fig. 9, outlier point ignored), the dimensionless wave number used in Fig. 1 can be calculated as:

$-2\pi y/SL = 1.0 \cdot 10^2$ to $6.5 \cdot 10^2$ if the waves are in the kinematic band, or

$-2\pi y/SL = 2.1 \cdot 10^1$ to $1.2 \cdot 10^2$ if the waves are in the gravity band

Comparing these results with the second graph of Fig. 1 (F = 0.10) suggests that only the second-row range (gravity band) is compatible with the wave theory. It can be further shown that the measured waves could not have been in the ice coupled or acoustic bands. According to Steffler and Hicks (1994), ice-coupling begins to have an effect on the wave celerity when the wavelength drops below a limiting value, L_i, that is given by:

$$L_i \approx \frac{16.7\ell}{(1+F)^{1/4}} \qquad (4)$$

At the time of the measurements, the ice cover was approximately 0.20 m thick and had already been subjected to considerable thermal deterioration. Consequently, the value of E is taken as 1.0 GPa (as opposed to 6.8 GPa for undeteriorated ice). The characteristic length, ℓ, is thus calculated as 3.0 m, using Eq. 2. With F = 0.10, L_i then works out to be 49 m. Since the wave celerity is still very close to that of the gravity band (see also Fig. 1), the corresponding period is about 10 s, which is well below the measured wave periods (70 or more seconds).

Consequently, it is concluded that all measured waves, with the possible exception of the outlier in Fig. 9 were in the gravity band, for which the celerity is approximately equal to 3.8 or 4.7 m/s, depending on whether the wave is propagating upstream or downstream. Using Eq. 3, the range of wavelengths is estimated as L ≈ 270 – 1500 m.

6.2. Ice Fracturing Capacity of Observed Waves

According to Daly (1995) the minimum amplitude of a sinusoidal water wave that is required to cause a transverse crack is given by:

$$a_{\min} = \frac{2\sigma(1-\nu^2)}{Eh_i}\left(\frac{L}{2\pi}\right)^2\left\{1+\left(\frac{2\pi\ell}{L}\right)^4\right\}\left\{1-\left(\frac{C}{C_H}\right)^2\right\} \qquad (5)$$

in which σ = flexural strength of the ice cover; and C_H = "free" or "homogeneous" wave celerity, a parameter that is much greater than C in the kinematic, dynamic, and gravity bands. Consequently, $1-(C/C_H)^2 \approx 1$. With $\ell \approx 3$ m and L = 270-1500 m, as calculated earlier, the ratio

$2\pi\ell/L$ is in the range 0.01 to 0.07. The term $(2\pi\ell/L)^4$ can thus be neglected relative to 1 in Eq. 4, which simplifies to:

$$a_{\min} \approx \frac{2\sigma(1-\nu^2)}{Eh_i}\left(\frac{L}{2\pi}\right)^2 \qquad (6)$$

With the estimated values of L (270-1500 m), and with σ as low as 60 kPa (about one-tenth of the undeteriorated strength) a_{min} works out to be 1.1 to 31 m. These figures are orders of magnitude greater than the observed amplitudes (0.02 m or less), hence the measured waves could not possibly have fractured the ice cover.

It is emphasized that the amplitudes appearing in Eqs 5 and 6 refer to the water waves, and may differ from the respective amplitudes of the flexural ice waves that are directly responsible for fracture. For the present data, however, it can be shown that the theoretical solution (Daly, 1995) results in approximate equality between these two amplitudes [essentially because both $(C/C_H)^2$ and $(2\pi\ell/L)^4$ are much less than 1].

The lack of ice-fracturing capacity of the measured waves is further corroborated by the observed spacing of the transverse cracks, which is of the order of hundreds of metres, and much greater than the spacing which would result from wave-induced bending. When a flexural wave that can fracture the cover travels in the downstream or upstream direction, each successive crack produces a free-edge structural condition that requires both the local shear force and the bending moment to vanish. With this restriction, the next location of maximum bending moment is controlled by the edge, and can only amount to a few characteristic lengths (e.g. see Hetenyi, 1946). Since $\ell \approx 3$ m, waves-induced cracks would have been spaced at intervals of the order of 10 m, which is much less than the observed spacing.

6.3. Possible Cause of Observed Waves

As mentioned earlier, the causes of the observed waves are unknown at present. The following mechanism is considered a possible candidate, subject to future verification with additional field data. When transverse cracks form, the ice cover is divided into consecutive ice sheets of varying length. Their mobility increases with rising river stage and enlarged water surface width, and with gradual melting due to positive heat fluxes. Depending on local channel conditions, certain ice sheets may move for a short distance before being arrested by stationary sheets downstream. That such brief movements do occur is manifested by small pressure ridges at crack locations (e.g. see Fig. 6), or by rapid development of sizeable open-water sections between sheets.

Initially, a mobile ice sheet accelerates under the action of the flow shear stress, which is dictated by the velocity differential between water and ice. The discharge under the sheet increases slightly, to a value that partly depends on the available length of travel. When the latter is exhausted, the moving sheet impacts on the stationary sheet downstream and decelerates to zero velocity. The deceleration phase is relatively abrupt, owing to the large resistance produced by the crushing strength of ice. The discharge will have to decrease again to the pre-movement value throughout the length of the sheet. To satisfy the equations of motion, such disturbances in

flow conditions must be accompanied by perturbations in the water surface, that can then propagate in the form of waves.

While this reasoning is speculative, and subject to confirmation with future field data, it would explain the appearance of transverse cracks in the study reach before any significant waves were recorded. It would also be consistent with the positive correlation between amplitude and period (or wavelength), since both would then be related to the size of the wave-generating ice sheet.

7. Future Work

Though the present findings have answered some of the questions raised by previous theoretical works, they are only a first step toward documenting the role that under-ice waves play in the process of breakup. Since the waves recorded before breakup appear to be incapable of fracturing the ice cover, it would be desirable to extend the monitoring period right through the breakup event. This would enable documentation of far steeper waves, as ice jams begin to form and release.

For the present data set, assessment of the wavelength has relied on well-established, but still theoretical, knowledge concerning the wave celerity – wave number variation. More direct, and reliable, is in situ measurement of celerity. This can be achieved by simultaneous recording with two transducers, separated by a distance sufficient to produce measurable time shifts in otherwise identical signals. Not only would this approach provide a direct measure of the celerity of each wave form, but would also identify the associated direction of travel, which can be either upstream or downstream for most waves of interest.

8. Summary and Conclusions

Using specially designed monitoring equipment, theoretically postulated pre-breakup river waves have been detected and described for what appears to be the first time. The recorded waves were approximately sinusoidal in shape, and rather flat (amplitude of about 2 cm or less; wavelength of 270 –1500 m). A general trend for amplitude to increase with wavelength was detected, possibly resulting from the mechanism of wave formation. Despite considerable thermal deterioration of the ice cover, it was calculated that the recorded waves could not have caused the numerous transverse cracks that were observed during the pre-breakup period. It is recommended that future measurements extend beyond the pre-breakup phase in order to record larger waves that may be associated with ice jam releases. Simultaneous deployment of two pressure transducers would enable in situ determination of wave celerity and direction of propagation.

9. References

Balmforth, N.J. and Craster, R.V. 1999. Ocean waves and ice sheets. J. Fluid Mech., Vol. 395, 89-124.

Beltaos, S. 1990. Fracture and breakup of river ice cover. Canadian Journal of Civil Engineering, 17(2), 173-183.

Beltaos, S. 1995. Breakup of river ice. National Water Research Institute Contribution 95-125, Burlington, 88 p. Prepared as Chapter 5 for “River Ice Processes and Hydraulics”, a book to be edited by H.T. Shen under the sponsorship of IAHR.

Beltaos, S. 1997. Onset of river ice breakup. Cold Regions Science and Technology, Vol. 25, No. 3, 183-196.

Billfalk, L. 1982. Break-up of solid ice covers due to rapid water level variations. U.S. Army CRREL Report 82-3, Hanover, N.H, U.S.A., 24 p.

Daly, S.F. 1993. Wave propagation in ice-covered channels. Journal of Hydraulic Engineering, ASCE, 119(8), 895-910.

Daly, S.F. 1995. Fracture of river ice covers by river waves. Journal of Cold Regions Engineering, ASCE, 9(1), 41-52.

Hetenyi, M.1946. Beams on elastic foundation. The University of Michigan Press, Ann Arbor, Mi., USA; also John Wiley & Sons Canada Ltd, Rexdale, Canada.

Ponce, V.M. and Simons, D.B. 1977. Shallow wave propagation in open channel flow. Journal of the Hydraulics Division, ASCE, 103(HY12), 1461-1476.

Steffler, R.M. and Hicks, E.F. 1994. Discussion of "Wave propagation on ice-covered channels", Journal of Hydraulic Engineering, ASCE, 120(12), 1478-1480.

Xia, X. and Shen, H.T. 1999. Interaction of shallow water waves with ice cover. Report 99-3, Department of Civil and Environmental Engineering, Clarkson University, Potsdam, NY, USA.